Annu. Rev. Earth Planet. Sci. 2000. 28:141–67

UNDERSTANDING OBLIQUE IMPACTS FROM EXPERIMENTS, OBSERVATIONS, AND MODELING

E. Pierazzo and H. J. Melosh
Lunar and Planetary Lab., University of Arizona, 1629 E. University Blvd., Tucson, Arizona 84721; e-mail: betty@lpl.arizona.edu, jmelosh@lpl.arizona.edu

Key Words oblique impacts, impact angle, ejecta distribution, ricochet, hydrocode simulations

■ **Abstract** Natural impacts in which the projectile strikes the target vertically are virtually nonexistent. Nevertheless, our inherent drive to simplify nature often causes us to suppose most impacts are nearly vertical. Recent theoretical, observational, and experimental work is improving this situation, but even with the current wealth of studies on impact cratering, the effect of impact angle on the final crater is not well understood. Although craters' rims may appear circular down to low impact angles, the distribution of ejecta around the crater is more sensitive to the angle of impact and currently serves as the best guide to obliquity of impacts. Experimental studies established that crater dimensions depend only on the vertical component of the impact velocity. The shock wave generated by the impact weakens with decreasing impact angle. As a result, melting and vaporization depend on impact angle; however, these processes do not seem to depend on the vertical component of the velocity alone. Finally, obliquity influences the fate of the projectile: in particular, the amount and velocity of ricochet are a strong function of impact angle.

INTRODUCTION

Impacts have created enormous scars on the surfaces of nearly all solar system bodies, prompting Shoemaker (1977) to state that ''impact of solid bodies is the most fundamental process that has taken place on the terrestrial planets.'' As a result, in past decades a large amount of work, both experimental and theoretical, has been devoted to understanding details of the impact process. A great deal has been extracted from remote observations of impact craters on planetary surfaces (e.g. Smits & Sanchez 1973, Pike 1974, Cintala et al 1977, Hale & Head 1979, Schultz & Lutz-Garihan 1982, Schultz 1992, Wilhelms 1992), whereas laboratory-scale experiments have been most useful for clarifying aspects of impact processes such as crater excavation and ejecta emplacement (e.g. Gault 1973, Stöffler et al 1975, Gault & Wedekind 1978, Schultz & Gault 1990). Scaling laws have been derived to describe impact crater size, shape, depth, ejecta, and melt deposits as functions of impact speed and impactor size and type (e.g. Croft 1985, Schmidt & Housen 1987, Holsapple & Schmidt 1987). An important

parameter that has often been neglected in the study of impact craters is the angle of impact. Theoretically, it is well established that meteoroids impact planetary bodies along oblique trajectories (e.g. Gilbert 1893, Shoemaker 1962). The general connection and comparison between impact and explosion cratering (e.g. Shoemaker 1962, Baldwin 1963, Roddy 1977), together with the realization that most oblique hypervelocity impacts produce circular craters (Gault & Wedekind 1978), has conveyed the general notion that vertical impacts are a good representation of typical planetary impact events. The problem was exacerbated by the paucity of experimental facilities capable of varying the angle of impact and by computer limitations in handling the complexity of numerical modeling of oblique impacts. Recently, however, the study of oblique impacts has received renewed attention (e.g. Schultz 1996a; Schultz & D'Hondt 1996; Pierazzo & Melosh 1999a, 2000b).

A note of caution is necessary at this point: by definition, ''oblique impact'' is indicative of any nonvertical impact. Among the scientific community, the term has become a synonym for impacts at very low angles; in this review, however, the term oblique impact is used in its full meaning, whereas ''highly oblique impacts'' designates very low impact angles.

PROBABILITY OF OBLIQUE IMPACT

For an isotropic flux of impacting meteoroids it can be shown that regardless of the target planet's gravitational field, the probability of an impact at an angle between θ and $\theta + d\theta$, where θ is measured from the vertical, is

$$dP = 2 \sin \theta \cos \theta \, d\theta. \quad (1)$$

Nongravitating Bodies

Gilbert (1893) was the first to derive the probability of impact for oblique impacts for nongravitating bodies. Consider a meteoroid approaching a planetary body of radius R_B (see Figure 1*a*). The meteoroid strikes the planetary surface when its path brings it inside the cross section of the planetary body. The overall probability associated with this event is proportional to the cross section of the planetary body and the flux of meteoroids F:

$$P = \pi R_B^2 F.$$

The probability that the meteoroid passes at a distance x from the center of the cross section is given by

$$dP = 2\pi x F \, dx, \quad (2)$$

where by an elementary trigonometric theorem $x = R_B \sin\theta$ ($dx = R_B \cos\theta \, d\theta$),

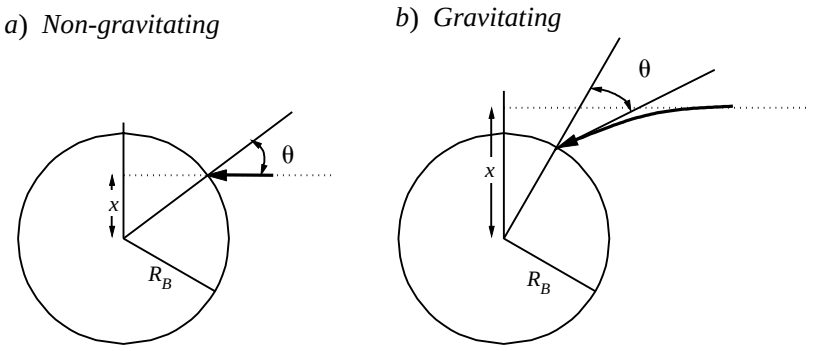

Figure 1 Diagram illustrating impact angle, θ, for bodies approaching a planetary body (radius R_B) without (*a*) and with (*b*) a gravitational field.

and θ is the angle of impact measured from the normal to the surface (zenith angle). Substituting in Equation 2,

$$dP = 2\pi R_B^2 F \sin\theta \cos\theta \, d\theta.$$

Normalizing by the probability of impacting anywhere on the planet, $P = \pi R_B^2 F$, we obtain Equation 1:

$$dP = 2 \sin\theta \cos\theta \, d\theta.$$

Gravitating Bodies

Shoemaker (1962) adapted Gilbert's derivation to take into account the gravitational attraction of a planetary body. When gravitational attraction is considered, the derivation uses the law of conservation of the angular momentum for a central force. Assume that the planetary body has a significant gravitational field (Figure 1*b*). Then the meteoroid is deflected by the planet's gravitational field. An impact occurs if the meteoroid is within the capture cross section of the planetary body. The probability for this to happen is $P = \pi R_g^2 \mathrm{F}$, where $R_g = \sqrt{1 + (v_{esc}/v_\infty)}$ (v_{esc} is the planet's escape velocity and v_∞ is the velocity of the meteoroid at infinite distance from the planet). Following the same reasoning above, we obtain again $dP = 2\pi x \, F \, dx$, where x is now the impact parameter.

The angular momentum is defined as $\mathbf{L} = m\mathbf{r} \times \mathbf{v}$, where m is the meteoroid mass, $\mathbf{v}$ is its velocity, and $\mathbf{r}$ is the distance from the planet. Using the law of conservation of angular momentum, then,

$$m \, R_\mathrm{B} \, v_i \sin\theta = m \, x \, v_\infty, \qquad (3)$$

where v_i is the meteoroid's impact velocity. Solving for x,

$$x = \frac{R_B v_i}{v_\infty} \sin \theta,$$

and substituting in Equation 2,

$$dP = 2\pi \frac{R_B v_i}{v_\infty} \sin \theta \frac{R_B v_i}{v_\infty} \cos \theta \, d\theta = 2\pi \left(\frac{R_B v_i}{v_\infty}\right)^2 \sin \theta \cos \theta \, d\theta.$$

From the law of conservation of energy, $v_i = \sqrt{v_\infty^2 + v_{esc}^2}$ and the term in parentheses becomes $R_B \sqrt{1 + (v_{esc}/v_\infty)^2} = R_g$. Normalizing by the probability of impacting anywhere on the planet, $P = \pi R_G^2 F$, we obtain again

$$dP = 2 \sin \theta \cos \theta \, d\theta.$$

Therefore, according to Equation 1, the angle of impact of maximum frequency is 45°, whereas the probability of vertical ($\theta = 90°$) as well as grazing ($\theta = 0°$) impacts is negligible.

The integral of Equation 1 predicts that 50% of impacts occur for θ between 30° and 60°, increasing to 76.6% for impacts between 20° and 70°. Highly oblique impacts, which may produce elliptical craters ($\theta < 15°$; see the ''Experimental Studies of Oblique Impacts'' section, later in this article) have a probability of occurring of about 6.7%, whereas the probability of grazing impacts, with $\theta < 5°$, is only about 0.75%.

HISTORICAL PERSPECTIVE

Although the study of impact cratering is relatively new, large craters, especially those on the Moon, have fascinated scientists for centuries, starting with Galileo in the sixteenth century. Since Galileo's initial discovery, lunar craters have been under scrutiny to the present day. For the longest time, lunar craters were believed to be volcanic in origin (e.g. Hooke 1665, Schröter 1791, Beer & Mädler 1837, Dana 1846, Herschel 1849, Nasmyth & Carpenter 1874). The first serious attempt to attribute an impact origin to the lunar craters came from Gilbert (1893), who studied them from a geologic perspective and concluded that they had to be formed by impact. He was the first to recognize a crater size-morphology relation, and he tabulated data on depth/diameter ratios. To support his idea, Gilbert also carried out low-velocity impact experiments.

A major problem with the impact hypothesis for the lunar craters, however, was the observation that the rims of nearly all lunar craters are circular. The low-velocity impact experiments carried out by Gilbert and many other scientists (see Baldwin 1978 for an overview) indicated that circular craters are produced only in vertical (or near vertical) impacts, whereas oblique impacts always produced elliptical craters, elongated in the direction of flight. Thus, attributing an impact origin to the lunar craters was equivalent to assuming that almost all impacts on the Moon were near vertical, a proposition that was correctly dismissed with

ridicule by early astronomers. Gilbert himself showed that probability theory points to 45° as the most probable angle of impact, whereas vertical and grazing impacts are rare.

An impact origin for lunar craters was therefore dismissed for a few decades more, until Gifford (1924) showed the connection between high-velocity impacts and explosions. Gifford pointed out that the angle of impact would not be important because ''whenever a meteorite penetrates into the crust the marks of ingress are completely blown away by the resulting explosion. Whatever the angle at which the meteorite strikes the surface, the explosion acts radially outward.'' Similar explanations were given by Öpik (1916) and Ives (1919) several years earlier but for various reasons failed to reach mainstream astronomers. Gifford's idea found more and more support in the following years, thanks to the increased exploration of terrestrial impact craters; by the end of the 1950s, the impact origin for lunar craters was widely accepted.

In recent years space exploration has provided a wealth of images of cratered surfaces of planetary bodies, from the large terrestrial planets to small asteroids. A common feature of these craters is that the majority of them are indeed circular. During these years our understanding of the impact process has improved dramatically as well. A fundamental contribution to our understanding of the relation between circular craters and oblique impacts was made by the experimental work carried out at the Ames Vertical Gun Ballistic Range (AVGBR) facility. Originally conceived by AC Charters, the gun was brought into operation in 1965 by DE Gault. The ensuing work by Gault and his coworkers proved that high-velocity impacts result in circular craters for most impact angles, with the exception of very oblique impacts ($<10°$–$15°$, measured from the surface). By solving the crater shape conundrum, this work paved the way to the universal acceptance of the impact origin of the Moon's craters.

EXPERIMENTAL STUDIES OF OBLIQUE IMPACTS

Experimental studies of oblique impacts date back to the simple, low-velocity impact experiments of Gilbert (1893). Similar low-velocity experiments were performed in the following decades. Only in the 1950s, however, were scientists able to carry out real hypervelocity impact experiments. The first hypervelocity oblique impacts were conducted by Rinehart & White (1951), who reached speeds up to 4.7 km/s with iron and aluminum projectiles impacting plaster-of-paris targets. However, the most comprehensive work on oblique impacts for geologic applications was carried out at the AVGBR facility.

Crater Shape

The first comprehensive study on crater shape was published by Gault & Wedekind (1978). To take into account the decrease in effective rock strength at planetary scales (gravity-dominated regime), as compared with laboratory scales, Gault &

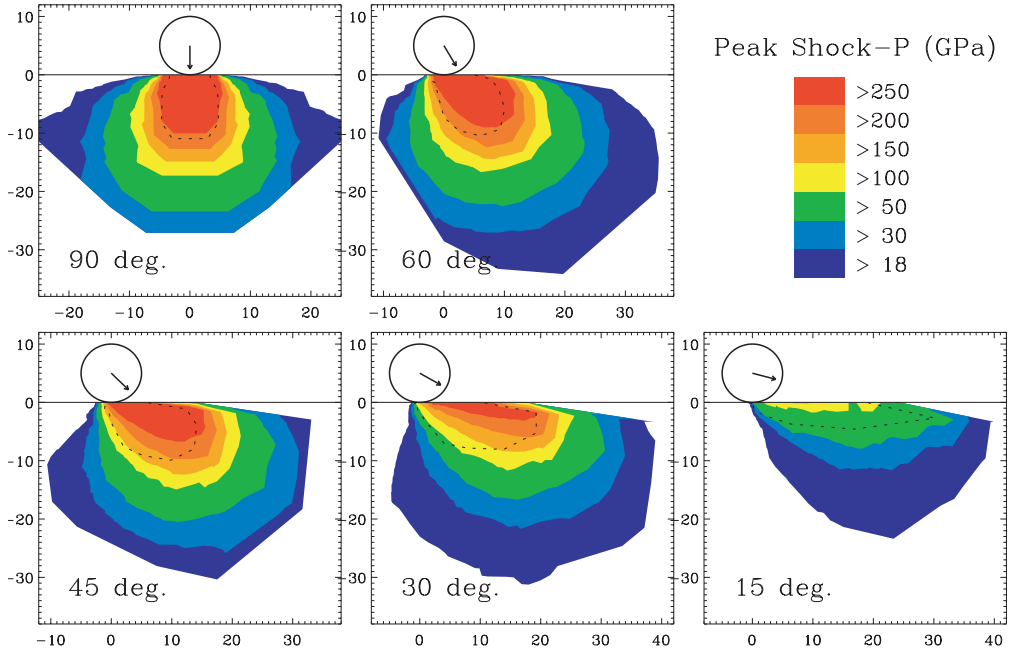

Figure 3 Peak shock pressure contours in the plane of impact for a series of 3D hydrocode simulations at various impact angles. *Dashed black line* represents the isobaric core. The projectile, 10 km in diameter, is shown for scale. *Vectors* illustrate the direction of impact. From Pierazzo & Melosh (2000b).

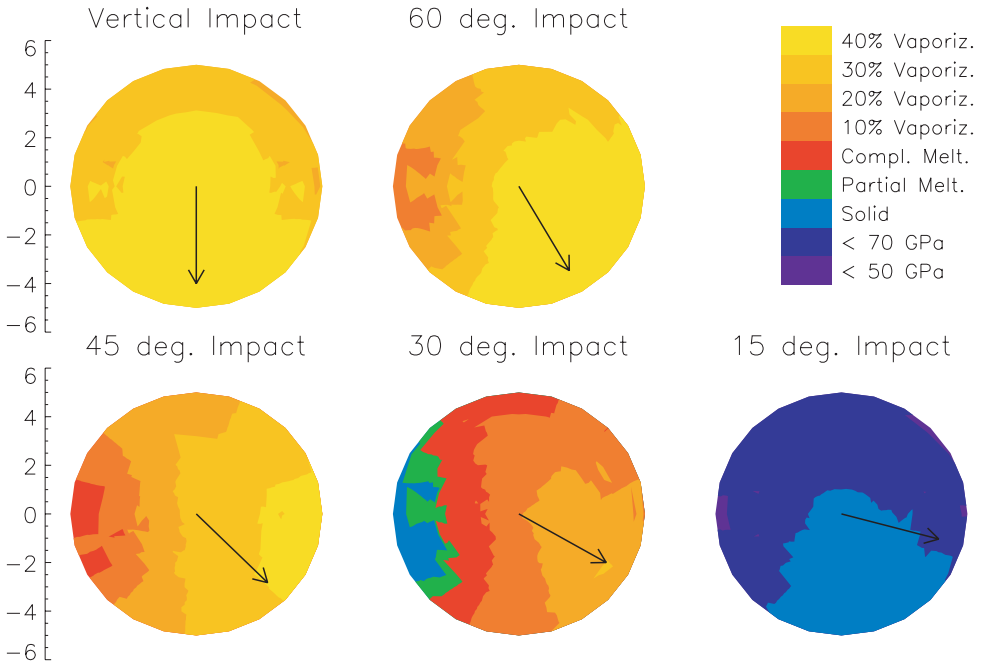

Figure 4 Distribution of melting and vaporization inside the dunite projectile for the various 3D hydrocode simulations. The maximum peak shock pressures corresponding to the various contours are: Solid = 135 GPa; Partial Melting = 149 GPa; Complete Melting = 186 GPa; 10% Vaporiz. = 224.5 GPa; 20% Vaporiz. = 286.5 GPa; 30% Vaporiz. = 363 GPa; 40% Vaporiz. = 468 GPa; 50% Vaporiz. = 437.2 GPa. From Pierazzo & Melosh (2000a).

Wedekind used particulate targets as the most representative for modeling large planetary cratering events. An advantage of this choice of targets is that the experiments are also directly applicable to small-scale regolith cratering. Gault & Wedekind's detailed work finally solved the mystery of the circularity of most impact craters on planetary surfaces. They found that craters in all target media remain circular within a few percent for impact angles from the vertical to at least 30°. For angles less than 30°, impact velocity and target and projectile materials play a role in the shape of the crater. At typical laboratory impact velocities ($\leq$7 km/s), they found that craters in quartz sand (a material virtually cohesionless, with density of 1.7 g/cm^3) show a marked in-path elongation only for angles below 10°. A similar behavior occurs in pumice powder targets (with density averaging 1.05 g/cm^3, and some cohesion), but with an additional trend between 30° and 10°, where craters become elongated at angles across the trajectory path (they observe an elongation of about 15% for five craters at 15°). For crystalline granite targets, on the other hand, craters appear significantly elongated along the trajectory path at 15°.

Ejecta Distribution

Other aspects of crater morphology are affected by angle of impact. Gault & Wedekind (1978) found that for angles less than 30°, steeper interior slopes formed on the uprange wall of the craters. The ejecta deposits exhibit axial symmetry for impact angles down to at least 45°. As the impact angle decreases below 45°, however, ejecta deposits become asymmetric, and ''forbidden'' azimuthal zones appear for impact angles less than about 30°, first uprange, and then downrange of the crater. A characteristic ''butterfly wing'' pattern of ejecta develops in very oblique ($<$5°) impacts, in which most of the ejecta is thrown out perpendicular to the projectile's path. Recent experiments by Schultz (1999) on the ejecta distribution from oblique impacts in particulate targets at low impact velocities 1–1.5 km/s) show a focusing of high-velocity ejecta in the downrange direction for a 30° impact, whereas the low-velocity ejecta is distributed more evenly around the crater. Melt produced by the impact is affected by impact angle as well and shows a pronounced downrange focusing for angles less than 45°.

Since the work of Gault & Wedekind (1978), the characteristic bilateral symmetry of the ejecta around craters has become the diagnostic feature for the recognition of craters formed by oblique impacts on planetary surfaces; it also provides a criterion for determining the direction of approach of the impactor.

Crater Efficiency

Experimental work also indicates that the size of the final crater decreases with increasing obliquity. Although crater diameter is the natural choice to describe the size of a crater, it is not the best choice for elongated craters. To describe the size dependence on obliquity down to very low impact angles, Gault & Wedekind (1978) represented crater size by the mass of target material displaced by the

impact event. This quantity, normalized by the projectile mass, is also called crater efficiency (e.g. Schultz & Gault 1990). Gault & Wedekind (1978) found that for particulate targets (gravity regime) crater efficiency decreases as $\sin\theta$, whereas for crystalline targets (strength regime) it decreases as $\sin^2\theta$. These two different behaviors can be reconciled using existing scaling relationships for strength and gravity dominated regimes if the vertical component of the impact velocity, $v_i \sin\theta$, is used (e.g. Chapman & McKinnon 1986). Gault & Wedekind also point out that the reduction of cratering efficiency with obliquity is accompanied by an increase in the energy fraction carried away by the ricocheted projectile fragments and ejecta.

Fate of the Projectile

The final state of the projectile is strongly dependent on the angle of impact. Ricochet occurs when a significant fraction of the projectile rebounds from its initial point of contact on the target surface and continues downrange in a ballistic trajectory. Gault & Wedekind (1978) concluded that there is no unique critical impact angle for the onset of ricochet. However, they find that in laboratory experiments ricochet is imminent as the angle of impact approaches 30°, and is well developed at 15° for rock targets; for particulate targets, it approaches 15° with full development at 10°. Depending on the projectile strength, and with increasing impact velocity, ricochet may occur either with the projectile remaining intact, rupturing into several large fragments, or shattering into a myriad of small fragments. Moreover, Schultz & Sugita (1997) concluded that vaporization would start in the lower part of the projectile during penetration, where it mixes with the target along the interface. Schultz & Gault (1990) suggest that even very low angle impacts ($<2.5°$) by a comet 10 km in diameter would result in complete disruption, whereas an asteroid with an assumed strength of 1 kb would allow fragments as large as 4 km to survive impact for angles up to 5°–7.5°. Finally, Fe-Ni objects could survive a glancing event (Gault & Wedekind 1978).

An intriguing result of this experimental work is the realization that ricocheted fragments of the projectile can retain a significant portion of the impact velocity (Gault & Wedekind 1978). This result was further investigated by Schultz & Gault (1990) in connection with the Cretaceous/Tertiary (K/T) boundary impact event. Figure 2*a* (page 243) of Schultz & Gault's (1990) paper shows that ricocheted fragments from partial disruption at very low impact angles ($<10°$) retain 60%–80% of the initial impactor velocity. This implies that high-velocity objects ($v_i \geq$ 15–20 km/s) could ricochet with velocities exceeding the escape velocity of the Earth (11.2 km/s). Lower impact velocities, on the other hand, would favor suborbital trajectories of the ricocheted fragments. In this case, Schultz & Gault (1990) conclude that most of the kinetic energy from the initial impactor will be directly transferred to the atmosphere, therefore amplifying the effect of the impact on the environment.

Shock Wave

Dahl & Schultz (1998) investigated the effect of obliquity on the decay of shock pressure in the target. Using piezoelectric stress gauges, they recorded the shock stress histories for a number of experiments at impact angles of 90° and 30°, performed at the AVGBR facility. They found that pressure decay appears to follow an energy scaling in the downrange and downward direction, i.e. a slope of –3 in a log-log plot of pressure versus distance from impact point; in the uprange direction, however, they found a slope of –2, which should not be allowed by the point source solution theory of Holsapple & Schmidt (1987). Furthermore, Dahl & Schultz (1999) found that the momentum content of the shock wave shows no clear dependence on the vertical component of the impact velocity; this is particularly true in the downrange direction, where the momentum content of the wave seems to be a function of impact velocity alone.

Expansion Plume

Recently, Schultz (1996a) presented the results of further experimental work that investigated possible effects of obliquity in the K/T boundary event. Schultz conducted oblique impact experiments into highly volatile targets, such as dry ice, powdered carbonate and dolomite, and calcite crystals, to study the effects of vaporization in oblique impacts. He found that a vapor cloud develops early in low-angle impacts ($<30°$). This early time vapor cloud decouples from the later stage crater growth and moves ballistically downrange. Some containment and redirection of a portion of the vapor cloud by the impact cavity also produces a small plume in the uprange direction for very low ($\leq 15°$) impact angles. The presence of an atmosphere slows down the expansion of the vapor cloud.

Vaporization

An apparently puzzling result presented by Schultz (1996a) is that the vapor-cloud energy increases with increasing obliquity, which appears to be in conflict with the expected effect of decreasing peak shock pressure with impact angle. Schultz (1996a) concludes that this most likely reflects an enhancement in vapor production (compared to vertical impacts, he estimates up to 15–20 times more vapor for carbonates and up to 50–100 times more vapor for dry ice in 15°–30° impacts), and proposes frictional shear heating for the responsible mechanism. Frictional shear heating occurs along the projectile/target interface, which increases with obliquity, and is localized near the surface. Therefore, Schultz (1996a) concludes that the vapor generated in low-angle impacts originates mainly in a region near the surface. The theoretical study of Pierazzo & Melosh (1999a) indicates a qualitative agreement with this conclusion. By looking at the results of a series of three-dimensional hydrocode simulations (Pierazzo & Crawford 1998), Pierazzo & Melosh (1999a) found an increase in vaporization of the target's surface layer as the impact angle decreases; the vaporization reaches a

maximum for a 30° impact. Quantitatively, however, the conclusions of Pierazzo & Melosh (1999a) are quite different: They find a maximum increase in vapor production of only about a factor of two, in clear contrast with the 15- to 20-fold increase indicated by Schultz. It must be noted, however, that the hydrocode simulations did not include a strength model, and therefore they cannot treat frictional effects.

It is still not clear how the experimental results of Schultz (1996a) apply to planetary scale impacts. In particular, a major concern is how localized the effect of shear heating is. It is well known that shear heating tends to concentrate in narrow shear bands (Gruntfest 1963, Grady 1980), which relieve differential stresses in adjacent material and sharply reduce the apparent stress of the overall mass. Melting (or degassing), therefore, is confined to these bands only. The width of these shear bands is controlled by thermal conduction, and in a large-scale impact is only a few centimeters to a few meters wide. Unfortunately, centimeter-size shear bands at laboratory scales are large enough to encompass the entire projectile and much of the target, therefore giving the impression of an homogeneous distribution of shear heating. At planetary scales, the effect of shear heating is probably limited to the narrow shear bands, which results in a much smaller amount of melting or degassing.

THE PLANETARY RECORD OF OBLIQUE IMPACTS

The search for craters that show features typical of oblique impacts on planetary surfaces has always paralleled the experimental work on oblique impacts. Every planetary surface of the solar system contains craters with features characteristic of oblique impacts. Their study has led to a better understanding of the evolution of planetary surfaces.

Moon

The type example of very oblique impacts on planetary surfaces is the lunar crater Messier (e.g. Gault & Wedekind 1978). Messier is an elongated crater 14 × 6 km in size, located in Mare Fecunditatis, that displays a ''butterfly wing'' ejecta distribution similar to those formed in laboratory impacts at very low angles ($<5°$). The complex crater on the west of Messier, Messier A, could be a ricochet of Messier (Forsberg et al 1998), or it could be a preexisting crater that happened to be on the flight path of downrange ejecta from Messier (Nyquist 1984). Other features of Messier that have been used as indicative of grazing impact angles are a rim resembling a saddle with low region along the inferred impact direction and a median ridge along the length of the floor (Schultz & Lutz-Garihan 1982).

Few other craters with characteristics similar to Messier, i.e. formed by very oblique impacts, are observed on the Moon (e.g. see Gault & Wedekind 1978, Melosh 1989, Glotch et al 1999), a result consistent with probability theory. Cra-

ters from oblique impacts with angles up to 45°, however, are common. Recently, a study of 16 fresh lunar craters of various sizes (10–35 km in diameter) indicated that impacts between 15° and 45° consistently show a depressed rim in the uprange direction and an asymmetric ejecta pattern, whereas craters with symmetric ejecta blankets, suggestive of high-angle impacts, have nearly axisymmetric topographic shapes (Forsberg et al 1998).

Among large complex craters, Tycho (radius 85 km) is believed to have been formed by a very oblique impact. Schultz & Anderson (1996) suggest an impact angle less than 30°, based on the asymmetric distribution of ejecta. Tycho's ejecta blanket also displays a missing sector that is presumed to mark the uprange direction. They cite a subtle uprange offset of the central peak complex as an indication of oblique impact. This is based on the supposition that the uprange offset of the maximum central uplift corresponds to an uprange offset of maximum crater depth. Such an offset was observed in laboratory experiments at very low impact angles (<30°; Gault & Wedekind 1978).

Oblique impacts have been suggested for lunar basins. Asymmetries in the structure and ejecta deposits of the Imbrium and Orientale basins have led some authors (Baldwin 1963; Wilhelms 1987; Schultz 1995, 1996b) to propose that they were created by oblique impacts. In particular, Schultz (1995) suggests that the observed features of Imbrium can be explained by an impact angle around 30° (but not lower than 25°) and a direction from the northwest; a similar impact angle is also suggested for Orientale (Schultz 1996b). Analogously, Crisium basin presents features suggestive of a very low impact angle. Wilhelms (1987) points to a series of asymmetries similar to those observed for Messier, and concludes that this is suggestive of an oblique impact from the west, possibly by a fragmented body; Schultz (1996b) suggests an impact angle as low as 10°. A low-velocity (~5 km/s), low-angle (<30°) impact from the south of a large object (radius >10% of the lunar radius) has been proposed also for the formation of the South Pole Aitken Basin (Schultz 1997).

Mercury

Very little work on oblique impacts on Mercury appears in the literature. Asymmetries are observed around Mercurian craters, such as the two-ring basin Bach (Schultz 1994), but no systematic study of oblique impacts has been carried out for Mercury.

Mars

Many craters on Mars display the asymmetric ejecta pattern and elliptical crater form indicative of impact angle within 15° from the surface (Strom et al 1992). In particular, Schultz & Lutz-Garihan (1982) identify 176 probable grazing (<5°) impact craters (Messier-like) larger than 3 km in diameter in Viking images of Mars. This number corresponds to about 5% of the total crater population on Mars, and is similar to what was recently found for both the Moon and Venus

(Glotch et al 1999). However, this percentage is almost one order of magnitude larger than the theoretical predictions of the probability of impacts at angles less than 5° from the surface, for an isotropic flux of impactors. Although Schultz & Lutz-Garihan (1982) propose that the large number of Martian grazing impacts could be due to a swarm of satellites whose orbits tidally decayed in time, Glotch et al (1999) claim a less unique mechanism must be responsible for this discrepancy. They suggest that the similar large fraction of elliptical craters on Mars, the Moon, and Venus could be explained by revising the threshold incidence angle necessary to produce elliptical craters. Interpolating between impact experiment data produced in sand and aluminum, Glotch et al (1999) concluded that the new elliptical crater threshold angles for Venus, Mars, and the Moon are 13°, 15°, and 16°, respectively, which correspond to probabilities of 4%–5%, in agreement with the observations.

Recently, an oblique impact has been proposed for the formation of the Western Arabian Shelf (WAS), S-SE of the Chryse Basin (Frey & Roark 1998). The WAS is a low-lying region, with an unusually thin crust for a cratered terrain; it is also noticeably deficient in large craters in the 100- to 200-km diameter range. According to Frey & Roark (1998), endogenic processes alone, such as subcrustal erosion and subsidence, cannot account for these features. They propose that a low-angle impact from the northwest could have formed the Chryse Basin, and the ricochet could have continued in the downrange direction, resulting in an asymmetric excavation (mainly downrange) and the production of sibling impacts clustered downrange of the Chryse Basin.

Venus

Over 900 impact structures have been identified on the surface of Venus (Schaber et al 1992). On Venus, the impact cratering process is affected by the planet's dense atmosphere and high surface temperature (Ivanov et al 1992), making the Venusian cratering record ideal for assessing the effects of an atmosphere on impact crater formation (Schultz 1992). Impact structures on Venus also represent an important data set for studying the effects of impact angle on impact cratering. Venusian craters appear relatively pristine (e.g. Phillips et al 1992), and have clearly defined ejecta deposits that appear distinct from those on other planetary surfaces, possibly because they are deposited from a cloud or a debris flow (due to the presence of a thick atmosphere) rather than being ballistically emplaced (Herrick et al 1997). Moreover, many Venusian craters have outflows that extend well beyond the continuous ejecta blanket (Phillips et al 1992). The most comprehensive interpretation of these ejecta deposits is given by Schultz (1992). Other analyses have been presented by Asimov & Wood (1992), Chadwick & Schaber (1993), and Johnson & Baker (1994). Although the details of the formation mechanism of the outflows are still controversial, all the authors agree on the importance of impact angle in the generation and distribution of melt and vapor. It is believed that the more oblique the impact, the longer the outflow in the downrange

direction (Schultz 1992), although a recent statistical analysis of the Venusian cratering record does not seem to confirm this interpretation (RG Strom, personal communication). Figure 2 from Schultz (1992) illustrates the connection between impact crater features and impact angle on Venus. For grazing impacts (<5°–10°), such as crater Graham (190 × 50 km in size; Herrick et al 1997), the characteristic butterfly ejecta pattern appears to be displaced downrange, while long outflows cover a broad area in the downrange direction, unless redirected by slopes. For impact angles larger than about 5°–10°, the shape of the craters does not provide conclusive information on obliquity. Schultz (1992) uses the ejecta blanket to roughly identify the angle of impact as follows: 20° for craters with uprange forbidden zone of ejecta; 30° for craters with asymmetric ejecta but not forbidden zones; 50° for craters with slightly asymmetric ejecta; and 70° for angles with relatively symmetric ejecta facies.

Schultz (1992) suggests that the location of the central peak or peak ring is a further diagnostic feature of impact angle for complex craters. According to his analysis of Venusian craters and of few craters on other planetary surfaces (e.g. Tycho and King on the Moon; Schultz & Anderson 1996), for very low impact angles the central peaks tend to be offset uprange. This feature could be a useful

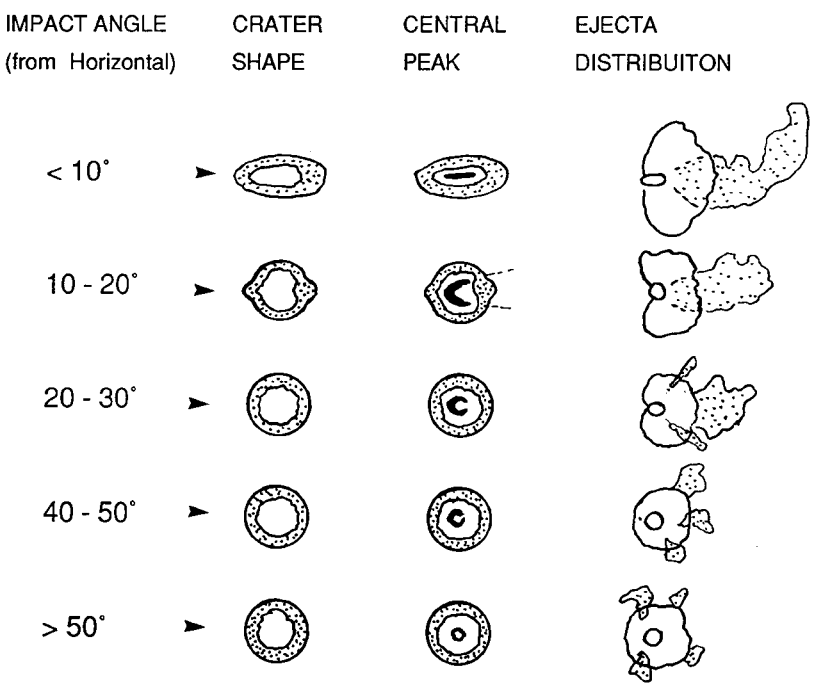

Figure 2 Diagnostic signatures of impact angle and direction based on laboratory experiments and craters on the Moon and Mars applied to Venus. From Schultz (1992).

tool for assessing impact angle for craters that do not have a well-preserved ejecta distribution, such as most terrestrial craters. Recently, however, this diagnostic feature has been questioned by Ekholm (1999). After analyzing some 39 complex Venusian craters, Ekholm (1999) finds an average uprange offset of the central peak complex of only 0.005 crater diameters, virtually indistinguishable from a random Gaussian distribution. Schultz's (1992) suggestion that the central peak is centered above the deepest part of the transient crater, uprange of the crater's center, is probably valid. However, it appears that later crater collapse and modification act to eradicate any evidence of this initial offset. This conclusion is confirmed by the work of Herrick & Forsberg (1998). They found that the large crater Manzolini (50 $\times$ 36 km), with the oblong shape characteristic of very low impact angles (they suggest $\sim$1°), has a symmetric central peak centered within the crater. Herrick & Forsberg (1998) also found that, while a clear correlation exists between impact angle and crater depth for small Venusian craters ($\sim$5 km in diameter), the variation of depth with impact angle is much less pronounced for larger craters. They attribute this depth/impact angle correlation for small craters to the fragmentation of the meteoroid in the dense Venusian atmosphere. Fragmented impactors are presumed to make shallower craters. Moreover, Herrick & Forsberg (1998) found a depressed or nonexistent rim in the uprange direction for craters inferred to have impact angles of 15°–45°, as is also observed in lunar craters (e.g. Forsberg et al 1998). This seems consistent with the experimental results of Gault & Wedekind (1978; see their Figure 5). The connection between impact angle and rim height, however, is still under debate. Indeed, Schultz & Anderson (1996) consider the lowest rim height to indicate not the uprange but the downrange direction, citing data for the craters Torricelli and Messier on the Moon and Manson on the Earth to support their claim.

Earth

The highly active geologic environment of the Earth removes and obscures impact craters. As a result, only about 150 impact structures have been recognized on Earth so far (Grieve 1997), a very small number compared with other planetary bodies of the solar system. Although the investigation of terrestrial craters has proved to be invaluable for our understanding of impact cratering, the recognition of oblique impacts is not an easy task. Weathering and erosion tend to delete or obscure the ejecta distribution, thus eliminating the best tool for identifying the angle of impact. Moreover, very oblique impacts are smaller and shallower than normal impacts, and thus tend to be more easily obscured by subsequent erosion. The Rio Cuarto crater field, on the farmland of the Pampas, Argentina, is a series of oblong, rimmed depressions that have been ascribed an impact origin (Schultz & Lianza 1992). The largest structure is 4.5 $\times$ 1.1 km in size, followed by a slightly smaller adjacent pair, $\sim$3.5 $\times$ 0.7 km in size, about 11 km to the southwest. The characteristics of this crater field suggest a very low angle of impact ($<$5°) of an impactor about 150 m in diameter coming from the northeast (Schultz

& Lianza 1992). The largest depression could have formed when the projectile first impacted the surface, and the smaller depressions could have formed by ricocheted fragments striking the ground downrange. Two chondritic fragments (H4/H5 type chondrites) have been recovered from one of the Rio Cuarto depressions. The analysis of several glasses, petrographically resembling impactites from known impact craters, show abundant evidence for an impact origin (Schultz et al 1994). None of them show evidence for mixing with the underlying country rock, only 15–20 m below the surface. Schultz et al (1994) point out that the most fractionated samples were found to the south of the Rio Cuarto craters and may represent the highest velocity component directed downrange.

An oblique impact has been suggested for the Ries crater (24 km in diameter), in the southern part of Germany. Although little indication comes from the crater's morphology, the localized occurrence of the Moldavite tektites suggests that the Ries was formed by an oblique impact from the West (Newsom et al 1990). Moldavites are found East of the Ries at distances of 260–400 km. They have been classified as distant ejecta of the crater based on an age undistinguishable from that of Ries, and a composition indicative that they are derived from Tertiary fresh water sediments present at the surface of the target area.

An impact angle of about 30° has been suggested for the formation of the Manson structure (35 km in diameter) in northwestern Iowa, by Schultz & Anderson (1996). Some of the evidence for this conclusion is still controversial, however, because it is based on interior crater features such as central peak offset and rim uplift. Manson is a well-studied crater, for which gravity, magnetic, seismic, and core/well data are available (Schultz & Anderson 1996). Unfortunately, however, ejecta deposits beyond the uncollapsed crater rim appear to have been largely removed, with maybe one exception—the Crow Creek Member of the Pierre Shale formation. This formation, which Izett et al (1993) considered to be Manson's distal ejecta (they have virtually the same age), shows clear signatures of an impact out to distances of 500 km northwest of Manson, but presents only minor occurrences of melt (Witzke et al 1996). An oblique impact would reduce the thickness of the melting region (e.g. see Pierazzo & Melosh 1999a), while causing mainly vaporization of the shallow sedimentary sequences at Manson (Kieffer & Simonds 1980).

The latest and most controversial suggestion of a terrestrial crater representative of an oblique impact is the buried Chicxulub structure, in the Yucatán Peninsula, Mexico (Hildebrand et al 1991). The Bouguer gravity data available on the structure indicates an elongated central gravity high trending northwest, encircled by a horseshoe-shaped gravity low. The central gravity high closely correlates with high-resolution aeromagnetic data (Schultz & D'Hondt 1996). The slight offset of the central gravity high with respect to the 180-km-diameter gravity-defined ring led Schultz & D'Hondt (1996) to suggest an impact at 20°–30° from the southeast to the northwest. However, the same asymmetry in the gravity high led Hildebrand et al (1998) to suggest an impact at ~60° from the southwest to the northeast. These two very different conclusions are indicative of the danger

of reaching conclusions from an incomplete set of data, and also show how much there is still to learn about planetary oblique impacts.

MODELING STUDIES

Notwithstanding their fundamental role in the investigation of oblique impacts, laboratory experiments cannot achieve the impact velocities typical of planetary impacts. On the other hand, observational studies of craters on planetary surfaces provide only qualitative information on oblique impacts, especially when coupled with the results of laboratory experiments. The limits of the experimental/hands-on techniques, therefore, make numerical modeling a critical tool for the study of oblique impact events. A fair amount of numerical modeling of vertical impacts is available in the literature; so far, however, only limited numerical modeling work has explored the effects of obliquity in impact events.

In vertical impacts, the axial symmetry of the process allows the simplification of the model to two dimensions (2D). In nonvertical impacts, the axial symmetry is broken, and at most, bilateral symmetry can be used to simplify the calculations. More complex and computationally intensive three-dimensional (3D) hydrocodes then must be used. Until recently, however, the latter option has been practically inaccessible, due to the large CPU and disk space required to run 3D hydrocodes.

Early 2½D Simulations

Preliminary work in modeling oblique impacts involved the use of so-called 2½D simulations (Brown 1981, O'Keefe & Ahrens 1986). In 2½D simulations, a 2D plain-strain code is used to model oblique impacts. In this case, an impacting spherical object is represented by an infinitely long rod of circular cross section. Because of this approximation, 2½D simulations can only model the flow field in the plane of impact, whereas the distribution of ejecta away from the plane of impact cannot be addressed at all. Furthermore, 2½D simulations tend to overestimate the shock pressure by an approximate factor of two (Brown 1981, Melosh 1989).

The early 2½D simulations by Brown (1981) indicated that in the plane of impact the peak pressure distribution is still symmetric in oblique impacts, with the symmetry point (corresponding to the point of largest shock pressure) shifting downrange of the impact. Outside the plane of impact, 2½D simulations can be used for oblique impacts with the assumption that the peak shock pressure distribution (for a spherical projectile) still retains full rotational symmetry about the symmetry point (Brown 1981). However, the results from 3D simulations show that this is not the case (see Figure 2 of Pierazzo & Melosh 1999a); some results of the early 2½D simulations have nonetheless been reproduced by 3D modeling. For example, 3D simulations (see Pierazzo & Melosh 1999a, Figures 3, 4, and 5) confirm the results of O'Keefe & Ahrens (1986) that the crater appears shal-

lower as the impact angle decreases. Furthermore, they found that the downrange ejecta velocity increases significantly with obliquity, which has been confirmed by Pierazzo & Melosh (1999b).

3D Simulations

The first (and only, so far) systematic modeling work on oblique impacts was carried out by Pierazzo & Crawford (1998). They performed a series of high-resolution 3D simulations of a Chicxulub-scale impact, where the only impact parameter that was allowed to vary was impact angle. An in-depth analysis of the results of these simulations is presented by Pierazzo & Melosh (1999a,b, 2000a,b).

The 3D simulations were computed using the hydrocode CTH (McGlaun & Thompson 1990) coupled with the SESAME equation of state package (SESAME '83 1983). The simulations model a projectile 10 km in diameter striking the Earth's surface at a velocity of 20 km/s and at impact angles of 15°, 30°, 45°, 60°, and 90° (vertical) from the surface. A resolution of 50 cells per projectile radius (cells 100 m $\times$ 100 m $\times$ 100 m) was applied to a cubic region of 16 km on a size centered on the impact point, followed by a region of progressively lower resolution where cell size increased by a factor of 1.05 from the previous cell. Due to the bilateral symmetry of the simulations, only the $y > 0$ semispace is defined (the $y < 0$ semispace is its mirror image), limiting the mesh to about 15 million cells. Each simulation starts with the projectile already at the target surface (atmospheric entry is not modeled), and covers about 5 s of the impact event, enough time for the shock to propagate through the target and cause shock melting/vaporization. Available tabular (SESAME) equations of state were used for the simulations. Dunite is used for the projectile, to model an asteroid impact. The simulations model the Chicxulub impact event (Pierazzo & Crawford 1998); therefore, the target composition reflects the stratigraphy of the Chicxulub impact site in the Yucatán Peninsula, Mexico (e.g. see Pierazzo et al 1998, Pierazzo & Melosh 1999a). Up to 1000 Lagrangian tracer particles are regularly distributed in the target and the projectile; they move through the mesh recording the thermodynamic history of given material points as a function of time. Rows of equally spaced tracers are located at regular angular intervals, from both the vertical and the downrange direction, denoted as the *x*-axis.

Shock Wave in Oblique Impacts Pierazzo & Melosh (1999a, 2000a) found that even though the position of the shock front as it propagates through the target appears symmetric around the impact point, the strength of the shock is asymmetric, with the strongest shock in the downrange direction. This is reflected in Figure 3 (see color insert), which shows the peak shock pressure contours experienced by the target in the plane of impact for the various simulations. As a result, the isobaric core near the impact site and the regions of melting show a pronounced downrange component and a decreasing depth as the impact angle decreases. A similar result is found for the projectile (Pierazzo & Melosh 2000a).

Figure 4 (see color insert) shows the peak shock pressure contours in the plane of impact. As the angle of impact decreases, the shock in the projectile becomes asymmetric and weaker, resulting in a decrease in projectile melting and vaporization with impact angle. The results of the oblique impacts also show that the amount of projectile that is ejected early from the opening cavity increases with increasing obliquity. The ejection velocity also increases with obliquity; for very low impact angles ($\leq 30°$) a fraction of the projectile carries a velocity in excess of the Earth's escape velocity (Pierazzo & Melosh 1999b), a result in agreement with experimental studies (Gault & Wedekind 1978). To test the dependence of the shock strength on impact angle, Pierazzo & Melosh (2000a, 2000b) calculated the mean shock pressure and temperature inside the isobaric core and in the projectile for the various 3D simulations. The result, shown in Figure 5, indicates that the shock weakens with impact angle. In the projectile, the peak shock pressure appears to depend approximately on the sine of impact angle θ, similar to the behavior of the shock pressure in the target (Pierazzo & Melosh 2000a). Analogously, the peak shock temperature in both the projectile and the target decreases with impact angle, but its dependence on angle goes as $\sin^{3/2}\theta$.

The pressure-decay with distance from the impact point, which outside the isobaric core is represented by a power law, is complicated by the asymmetry of the shock wave. A similar result was found by Dahl & Schultz (1998; also see the ''Experimental Studies of Oblique Impacts'' section of this article). Pierazzo & Melosh (2000b) propose the use of a volumetric pressure-decay relation instead of the pressure-distance function commonly cited in vertical impacts or explosions. The pressure decay is thus characterized by the function $p(V)$:

$$p(V) = K \left(\frac{V_{<p}}{V_{proj}} \right)^{-n_v}, \quad (4)$$

where $V_{<p}$ is the volume of target material shocked above the shock pressure p; V_{proj} is the initial volume of the projectile; K is a constant; and n_V is the volume pressure decay constant, which is easily shown to correspond to one third of the more common linear pressure decay constant (Pierazzo & Melosh 2000b). The numerical computations show that for impact angles between 30° and 90°, the volume pressure decay exponent is nearly constant. A weighted average for the simulations in that range gave $n_V = 0.671 \pm 0.007$, in fairly good agreement with one third of the average estimate of the linear pressure decay constant for the same simulations (Pierazzo & Melosh 2000b).

Melting in Oblique Impacts The amount of shock melting in the target is a strong function of angle of impact. Pierazzo & Melosh (2000b) found that for typical rocks the amount of impact melt decreases with impact angle: For impacts from 90° to 45° the decrease is less than 20%, whereas for impacts at 30° the volume of melt drops to about 50% of the amount in a vertical impact, declining to less than 10% for a 15° impact. A simple energy scaling law for the melt

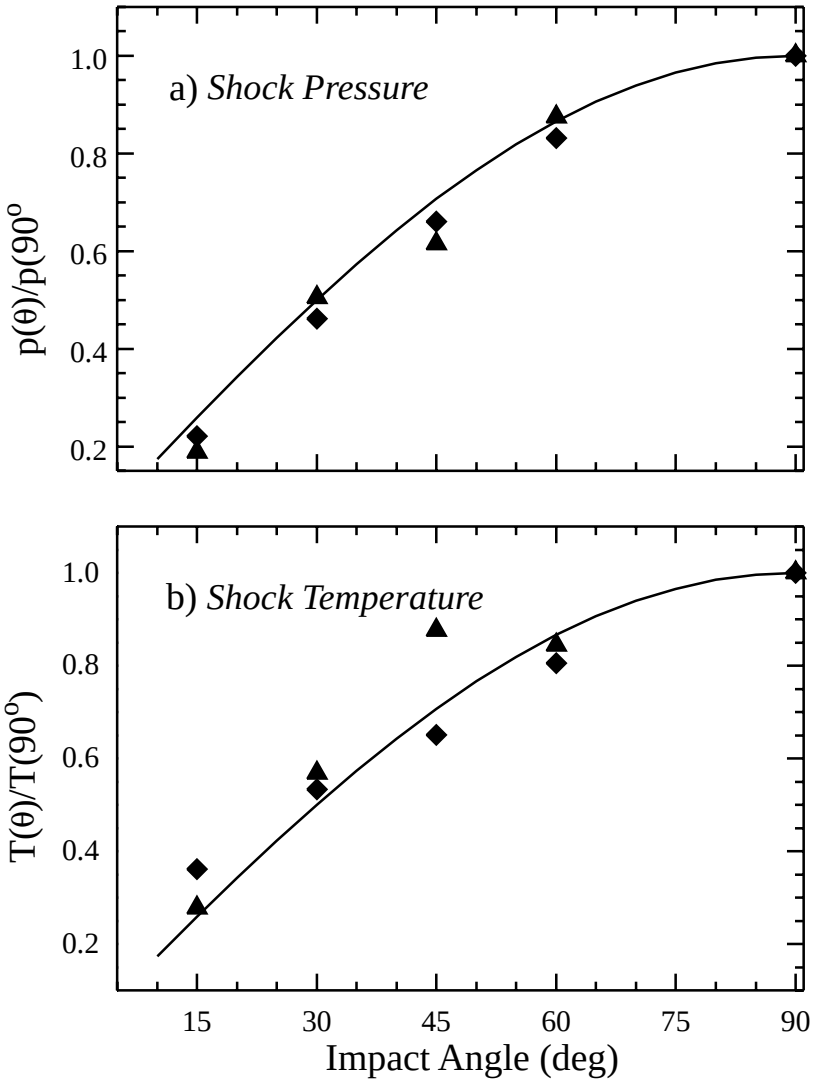

Figure 5 Mean peak shock pressures (*a*) and temperatures (*b*) inside the isobaric core (*diamonds*) and in the projectile (*triangles*) for the various 3D simulations as function of impact angle θ. For comparison, the *solid line* represents (a) sinθ and (b) $\sin^{3/2}\theta$.

volume is not applicable to oblique impacts. The amount of melt in oblique impacts is not a simple power of either the impact velocity or its vertical component (Pierazzo & Melosh 1999b). Therefore, Pierazzo & Melosh (2000b) suggest an approximate empirical scaling law. Experiments (Gault & Wedekind 1978)

showed that the volume of the transient crater is proportional to the vertical component of the impact velocity, $v_i \sin\theta$. If this is inserted into the scaling law from Schmidt & Housen (1987) for the volume of the transient crater excavated by the impact, the crater volume is given by

$$V_{tc} = 0.28 \frac{\rho_{pr}}{\rho_t} D_{pr}^{2.35} g^{-0.65} v_i^{1.3} \sin^{1.3}\theta, \quad (5)$$

where V_{tc} is the volume of the transient crater; ρ_{pr} and ρ_t are the densities of projectile and target, respectively (in kg/m^3); D_{pr} is the projectile diameter (in meters); and g is the acceleration of gravity (in meters per second). Using Equation 5, then, the volume of the transient crater can be estimated for the various oblique impact simulations.

In Figure 6, the volume of melt $V(>p)$ (where melting is assumed for pressures between 30 and 150 GPa), normalized to the volume of the transient crater, is plotted versus impact angle. With the exception of the 15° case, the ratio appears roughly constant. Given the large uncertainties associated with melt production, Pierazzo & Melosh (2000b) then conclude that for impact angles between 30° and 90° it is reasonable to assume that the volume of melt is directly proportional to the volume of the resulting transient crater. According to probability theory (see the ''Probability of Oblique Impact'' section of this article; Gilbert 1893, Shoemaker 1962) this conclusion applies to at least 75% of planetary-scale impact events.

APPLICATIONS TO GEOLOGIC PROBLEMS

Impact angle—especially low impact angle—is considered to have played a major role in various problems of geologic interest. Impact angle has long been proposed to be a critical parameter for the ejection of matter from planetary surfaces into interplanetary space (Nyquist 1984, O'Keefe & Ahrens 1986). Obliquity is also an important factor in the giant impact theory for the origin of the Moon (Hartmann et al 1986). The role of obliquity in increasing environmental effects for large planetary impacts has come under investigation (e.g. Pierazzo & Melosh 1999a, Schultz 1996a, Schultz & D'Hondt 1996, Pope et al 1997) as a result of the studies on the K/T boundary impact event.

Recently, a study on catastrophic impacts on asteroids has suggested that impact angle may play an important role for the final spin rate of asteroids (Love & Ahrens 1997). In particular, the Love & Ahrens (1997) results indicate that for the same degree of mass loss, low-angle impacts (15°) yield spin rates roughly twice those of impacts at 45°, which, in turn, have a spin rate roughly twice that of high-angle impacts (75°). Although still at the beginning stage, this work opens a new direction in studying the effects of obliquity in impact events.

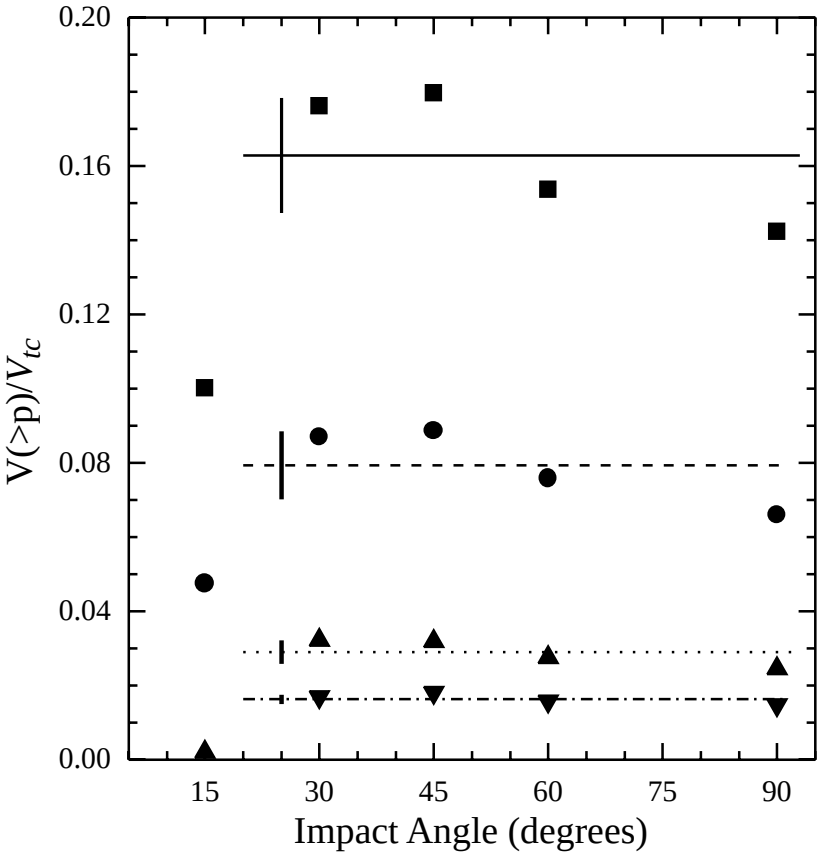

Figure 6 Ratio between volume of target material shocked above a given shock pressure, $V(>p)$, and volume of the resulting transient crater, V_{tc} ,versus impact angle. Shock pressures investigated are 30 GPa (*squares*), 50 GPa (*circles*), 100 GPa (*up-triangles*), 150 GPa (*down-triangles*). *Horizontal lines* represent the averages for the various shock pressures, for impact angles between 90° and 30°. *Vertical lines* represent 1-σ errors associated with the averages. (From Pierazzo & Melosh 2000b)

Oblique Impacts and Meteorites from Planetary Bodies of the Solar System

Since the realization that some of the meteorites originated from the surface of Mars and the Moon (e.g. Drake 1979, Wasson & Wetherill 1979, Walker et al 1979), impact cratering has become the most reasonable mechanism for ejecting material from planetary bodies of the Solar System. According to early studies (O'Keefe & Ahrens 1977), a small fraction of the matter involved in hypervelocity impacts on planetary surfaces can be accelerated to high velocities. Most of it,

however, is highly shocked material, which cannot account for the lightly shocked planetary meteorites that reached the Earth. Various impact-related mechanisms have been suggested as capable of launching lightly shocked ejecta from planetary surfaces, from spallation (Melosh 1983) to fluid drag (of an expanding vapor cloud; Wasson & Wetherill 1979, Vickery 1986). An alternative mechanism is a low-angle impact of large meteoroids (Nyquist 1983, 1984). Using the experiment results of Gault & Wedekind (1978) on ricochet velocities, Nyquist (1984) argues that only very oblique impacts could be able of ejecting material at velocities above the escape velocity of Mars or the Moon. He proposes 7° as the limit for escape from Mars, whereas the lower gravity on the Moon allows impact angles as high as 15°. O'Keefe & Ahrens (1986) addressed this problem with a series of 2½D simulations (see the ''Modeling Studies'' section of this article). Although they find that gas entrainment alone cannot provide a viable mechanism, they suggest that jetting could eject material at low shock levels and escape velocity. However, their work suggests that for impact angles below 25°, the ejecta jet contains only impactor material, because no substantial penetration of the planetary surface occurs. Only for angles above 25° does the high-speed ejecta also include planetary material. It is not clear, though, whether the speed of such ejecta is high enough for escape to occur. Furthermore, the development of a dense, fast gas jet tends to crush entrained solids and prevents the ejection of intact rocks (Vickery 1986). Recently, however, revised calculations on spallation by Head & Melosh (1999) have indicated that low impact angles may not be necessary to eject meteorites from the surface of Mars after all.

Origin of the Moon

The proposal that the Moon was created by a collision between the proto-Earth and a Mars-size protoplanet has gained many adherents in the past decade (Hartmann et al 1986). Such a planetary-scale collision was necessarily oblique, otherwise it could not have injected the angular momentum necessary to orbit the Moon. This problem can only be studied through the use of large 3D hydrocodes, because experiments in the field seem prohibitively expensive. Several numerical approaches have been used in the past: conventional Eulerian codes such as the Sandia CTH code (Melosh & Kipp 1989) and a new type of meshless Lagrangian hydrocode known as SPH (Smoothed Particle Hydrodynamics) (Benz et al 1989).

One of the outstanding problems in this field is the amount of Earth mantle material entrained in the material that eventually condenses into the Moon. Cameron, in his SPH models, finds that the impact must be so grazing that the Moon forms almost exclusively from the projectile (Benz et al 1989). Melosh & Kipp find that a few lunar masses of debris can be launched into orbit by a more central collision that produces large volumes of vapor through the jetting process and incorporates roughly equal masses of projectile and target (Melosh & Sonett 1986, Melosh & Kipp 1989). These two scenarios have different implications for the chemistry of an impact-created Moon. In addition, further computations are

needed to define the possible mass, approach angles, and velocity of the impacting protoplanet. Nevertheless, it is clear that the study of oblique impacts with complex geometry will be at the heart of dynamical studies of the Moon's origin for some time to come.

Oblique Impacts and Environmental Catastrophes

One of the major mass extinctions in the Phanerozoic (Sepkoski 1994), the Cretaceous/Tertiary mass extinction, has been associated with the impact event that formed one of the largest impact structures known on the Earth's surface, the Chicxulub structure in the Yucatán Peninsula, Mexico (Hildebrand et al 1991). Since then, a wealth of studies focused on the role of the impact in mass extinction (for a good review of the subject see Sharpton & Ward 1990, Ryder et al 1996). Recently, attention has been focused on the role of impact angle (e.g. Schultz 1996a, Schultz & D'Hondt 1996, Pope et al 1997, Pierazzo & Melosh 1999a) in the vaporization of highly volatile material from the sedimentary layer of the target region. It is believed that the release of climatically active gases into the atmosphere played a major role in the environmental catastrophe triggered by the impact event (e.g. Pope et al 1994, 1997; Pierazzo et al 1998). Pope et al (1997) used an ad hoc, geometrical approach to assess the role of impact angle. They used the projectile footprint to estimate the increase in volume of sediments degassed in an oblique impact. According to this correction, the volume of sediments degassed increases with the inverse of $\sin\theta$; it is at a minimum for a vertical impact, doubles for a 30° impact, and increases further at lower angles. Using 3D numerical simulations, Pierazzo & Melosh (1999a) conducted a more systematic study (see the ''Modeling Studies'' section of this article). They estimated the volume of sediments degassed at various impact angles from the distribution of the shock wave in the target (e.g. Figure 3). The result suggests a maximum increase of less than a factor of two for a 30° impact, with an abrupt drop for a 15° impact. Approaching the problem from the experimental point of view, Schultz (1996a) conducted oblique impact experiments on two-layer targets, with a highly volatile surface layer. His conclusions suggest a 10- to 15-fold increase in degassing of the sedimentary layer for low impact angles (15° and 30°), mainly due to shear heating (see the ''Experimental Studies'' section).

As discussed in the ''Experimental Studies'' section, the real effect of impact angle in the vaporization of target material is still under debate. Although it is improbable that more experimental work may solve the problem, further modeling work (that includes also a treatment of strength) may bring new insights to the debate.

CONCLUSION

Although the importance of obliquity was realized very early in the study of impact craters, real advances in studying the effects of impact angle have been made only in the face of great difficulties. Experimental studies required an elab-

orate facility, such as the Ames Vertical Gun Ballistic Range, that could launch fast projectiles at a variety of angles. Theoretical studies require massive 3D computer simulations that are only now becoming possible on a regular basis. Observational studies of the effects of impact angle on craters are fraught with biases and obscured by the presence of other poorly characterized physical processes.

It should be clear from the discussion in this review that there are still many points of disagreement between experiment, theory, and observation. Nevertheless, a great deal of progress has been made—much of it in the past decade. The outlook for significant advances in theoretical studies is especially bright because of the rapid increase in the capability of computer systems. The observational database is being extended by space missions. A great deal of useful data on oblique impacts is available in the Magellan data on Venus. Very-high-resolution images from Mars Global Surveyor may also be helpful in defining the properties of oblique impact craters.

Overall, we have made substantial progress in understanding the major effects of impact angle on cratering processes. We look forward to the resolution of some of the current controversies about the effects of impact angle, and hope that new applications, such as the effects of oblique impacts on asteroids or on the planetary-scale collision that may have formed the Earth's Moon, will arise.

ACKNOWLEDGMENTS

This work was supported by NASA grants NAGW-5159 and NAGW-428. We thank Dr. PA Schultz for providing Figure 2 of the manuscript.

LITERATURE CITED

Asimov PD, Wood JA. 1992. Fluid outflows from Venus impact craters: analysis from Magellan data. *J. Geophys. Res.* 97: 13643–66

Baldwin RB. 1963. *The Measure of the Moon.* Chicago: Univ. Chicago Press. 488 pp.

Baldwin RB. 1978. An overview of impact cratering. *Meteoritics* 13:364–79

Beer W, Mädler JH. 1837. *Der Mond.* Berlin: Schropp. 412 pp.

Benz W, Cameron AGW, Melosh HJ. 1989. The origin of the Moon and the single impact hypothesis III. *Icarus* 81:113–31

Brown WT. 1981. Numerical modeling of oblique hypervelocity impact using two-dimensional plane strain models. In *Shock Waves in Condensed Matter,* ed. WJ Nellis, L Seaman, RA Graham, pp. 529–33. New York: Am. Inst. Phys. 715 pp.

Chadwick DJ, Schaber GG. 1993. Impact crater outflows on Venus: morphology and emplacement mechanisms. *J. Geophys Res.* 98:29891–902

Chapman CR, McKinnon WB. 1986. Cratering of planetary satellites. In *Satellites,* ed. JA Burns, MS Matthews, pp. 492–580. Tucson: Univ. Ariz. Press. 1021 pp.

Cintala MJ, Wood CA, Head JW. 1977. The effects of target characteristics on fresh crater morphology: preliminary results for the Moon and Mercury. *Proc. Lunar Planet. Sci. Conf.* 8:3409–25

Croft SK. 1985. The scaling of complex craters. *Proc. Lunar Planet. Sci. Conf.* 15:C828–42

Dahl JM, Schultz PH. 1998. Shock decay in oblique impacts. *Lunar Planet. Sci. Conf. 29th*, Abstr. #1958. Houston, TX: Lunar Planet. Inst. (CD-ROM)

Dahl JM, Schultz PH. 1999. In-target stress wave momentum content in oblique impacts. *Lunar Planet. Sci. Conf. 30th*, Abstr. #1854. Houston, TX: Lunar Planet. Inst. (CD-ROM)

Dana JD. 1846. On the volcanoes of the Moon. *Am. J. Sci.* 52:335–55

Drake MJ. 1979. Geochemical evolution of the Eucrite Parent Body: possible nature and evolution of Asteroid 4 Vesta? In *Asteroids*, ed. T Gehrels, pp. 765–82. New York: Pergamon. 1181 pp.

Ekholm AG. 1999. Crater features diagnostic of oblique impacts: the central peak offset. *Lunar Planet. Sci. Conf. 30th*, Abstr. #1706. Houston, TX: Lunar Planet. Inst. (CD-ROM)

Forsberg NK, Herrick RR, Bussey B. 1998. The effects of impact angle on the shape of lunar craters. *Lunar Planet. Sci. Conf. 29th*, Abstr. #1691. Houston: Lunar Planet. Inst. (CD-ROM)

Frey H, Roark J. 1998. Origin of the Western Arabian Shelf: oblique impact formation of the Chryse Basin? *Lunar Planet. Sci. Conf. 29th*, Abstr. #1664. Houston: Lunar Planet. Inst. (CD-ROM)

Gault DE. 1973. Displaced mass, depth, diameter, and effects of oblique trajectories for impact craters formed in dense crystalline rocks. *Moon* 6:32–44

Gault DE, Wedekind JA. 1978. Experimental studies of oblique impacts. *Proc. Lunar Planet. Sci. Conf.* 9:3843–75

Gifford AC. 1924. The mountains of the Moon. *N.Z.J. Sci. Technol.* 7:129–42.

Gilbert GK. 1893. The moon's face, a study of the origin of its features. *Bull. Philos. Cos. Wash. (D.C.)* 12:241–92

Glotch T, Bottke W, Love S, Tytell D. 1999. The elliptical crater populations on the Moon, Mars, and Venus. *Lunar Planet. Sci. Conf. 30th*, Abstr. #1441. Houston: Lunar Planet. Inst. (CD-ROM)

Grady DE. 1980. Shock deformation of brittle solids. *J. Geophys. Res.* 85:913–24

Grieve RAF. 1997. Extraterrestrial impact events: the records in the rocks and the stratigraphic column. *Palaeogeog. Palaeoclimatol. Palaeoecol.* 132:5–23

Gruntfest IJ. 1963. Thermal feedback in liquid flow: plane shear at constant stress. *Trans. Soc. Rheol.* 7:195–207

Hale WS, Head JW. 1979. Central peaks in lunar craters: morphology and morphometry. *Proc. Lunar Planet. Sci. Conf.* 10:2623–33

Hartmann WK, Phillips RJ, Taylor GJ, eds. 1986. *Origin of the Moon.* Houston, TX: Lunar Planet. Inst. 781 pp.

Head JN, Melosh HJ. 1999. Effects of layering on spall velocity: numerical simulations. *Lunar Planet. Sci. Conf. 30th*, Abstr. #1761. Houston: Lunar Planet. Inst. (CD-ROM)

Herrick RR, Sharpton VL, Malin MC, Lyons SN, Feely K. 1997. Morphology and morphometry of impact craters. In *Venus II. Geology, Geophysics, Atmosphere, and Solar Wind Environment*, ed. SW Bougher, DM Hunten, RJ Phillips, pp. 1015–46. Tucson-London: Univ. Ariz. Press. 1362 pp.

Herrick RR, Forsberg NK. 1998. The topography of oblique impact craters on Venus and the Moon. *Lunar Planet. Sci. Conf. 29th*, Abstr. #1525. Houston: Lunar Planet. Inst. (CD-ROM)

Herschel JFW. 1849. *Outlines of Astronomy.* London: Longmans, Green. 620 pp.

Hildebrand AR, Penfield GT, Kring DA, Pilkington M, Jacobsen S, Boynton WV. 1991. A possible Cretaceous-Tertiary boundary impact crater on the Yucatan Peninsula, Mexico. *Geology* 19:867–71

Hildebrand AR, Pilkington M, Halpenny J, Cooper R, Connors M, et al. 1998. Mapping Chicxulub crater structure with overlapping gravity and seismic surveys. *Lunar Planet. Sci. Conf. 29th*, Abstr. #1821. Houston: Lunar Planet. Inst. (CD-ROM)

Holsapple KA, Schmidt RM. 1987. Point source solutions and coupling parameters in cratering mechanics. *J. Geophys. Res.* 92:6350–76

Hooke R. 1665. *Micrographia.* London: Martyn & Allestry. (A facsimile reproduction was published in 1961 by Dover Publ. of New York)

Ivanov BA, Nemchinov IV, Svetsov VA, Provalov AA, Khazins VM, Phillips RJ. 1992. Impact cratering on Venus: physical and mechanical models. *J. Geophys. Res.* 97:16167–81

Ives HE. 1919. Some large-scale experiments imitating the craters of the Moon. *Astrophys. J.* 50:245–50

Izett GA, Cobban WA, Obradovich JD, Kunk MD. 1993. The Manson impact structure: $^{40}Ar/^{39}Ar$ age and its distal impact ejecta in the Pierre Shale in southeastern South Dakota. *Science* 262:729–32

Johnson JR, Baker VR. 1994. Surface property variations in Venusian fluidized ejecta blanket craters. *Icarus* 110:33–70

Kieffer SW, Simonds CH. 1980. The role of volatiles and lithology in the impact cratering process. *Rev. Geophys. Space Phys.* 18:143–81

Love SG, Ahrens TJ. 1997. Origin of asteroid rotation rates in catastrophic impacts. *Nature* 386:154–56

McGlaun JM, Thompson SL. 1990. CTH: a three-dimensional shock wave physics code. *Int. J. Imp. Eng.* 10:351–60

Melosh HJ. 1983. Impact ejection, spallation and the origin of certain meteorites. *Lunar Planet. Sci. Conf.* 14:499–500

Melosh HJ. 1989. *Impact Cratering: A Geologic Process.* New York: Oxford Univ. Press. 245 pp.

Melosh HJ, Sonett CP. 1986. When worlds collide: jetted vapor plumes and the Moon's origin. See Hartmann et al 1986, pp. 621–42

Melosh HJ, Kipp ME. 1989. Giant impact theory of the Moon's origin: first 3-D hydrocode results. *Lunar Planet. Sci. Conf.* 20:685–86

Nasmyth J, Carpenter J. 1874. *The Moon: Considered as a Planet, a World, and a Satellite.* London: Murray. 189 pp.

Newsom HE, Graup G, Iseri DA, Geissman JW, Keil K. 1990. The formation of the Ries crater, West Germany; evidence of atmospheric interactions during a large cratering event. See Sharpton & Ward 1990, pp. 195–206

Nyquist LE. 1983. Do oblique impacts produce Martian meteorites? *Proc. Lunar Planet. Sci. Conf.* 13:A785–98

Nyquist LE. 1984. The oblique impact hypothesis and relative probabilities of lunar and Martian meteorites. *Proc. Lunar Planet. Sci. Conf.* 14:631–40

O'Keefe JD, Ahrens TJ. 1977. Meteorite impact ejecta: dependence of mass and energy lost on planetary escape velocity. *Science* 198:1249–51

O'Keefe JD, Ahrens TJ. 1986. Oblique impact: a process for obtaining meteorite samples from other planets. *Science* 234:346–49

Öpik E. 1916. Note on the meteoric theory of lunar craters. *Bull. Soc. Russe Amis Etude Univers (Mirove denie)* 5:125–34. (In Russian with French summary)

Phillips RJ, Raubertas RF, Arvidson RE, Sarkar IC, Herrick RR, et al. 1992. Impact craters and Venus resurfacing history. *J. Geophys. Res.* 97: 15923–48

Pierazzo E, Crawford DA. 1998. Modeling Chicxulub as an oblique impact event: results of hydrocode simulations. *Lunar Planet. Sci. Conf. 29th,* Abstr. #1704. Houston: Lunar Planet. Inst. (CD-ROM)

Pierazzo E, Kring DA, Melosh HJ. 1998. Hydrocode simulation of the Chicxulub impact event and the production of climatically active gases. *J. Geophys. Res.* 103:28607–25

Pierazzo E, Melosh HJ. 1999a. Hydrocode modeling of Chicxulub as an oblique impact event. *Earth Planet. Sci. Lett.* 165:163–76

Pierazzo E, Melosh HJ. 1999b. Melt production in oblique impacts. *Lunar Planet. Sci.*

Conf. 30th, Abstr. #1223. Houston: Lunar Planet. Inst. (CD-ROM)

Pierazzo E, Melosh HJ. 2000b. Melt production in oblique impacts. *Icarus.* In press

Pierazzo E, Melosh HJ. 2000a. Hydrocode modeling of oblique impacts: the fate of the projectile. *Meteorit. Planet. Sci.* 35(1): In press

Pike RJ. 1974. Depth/diameter relations of fresh lunar craters: revision from spacecraft data. *Geophys. Res. Lett.* 1:291–94

Pope KO, Baines KH, Ocampo AC, Ivanov BA. 1994. Impact winter and the Cretaceous/Tertiary extinctions. *Earth Planet. Sci. Lett.* 128:719–25

Pope KO, Baines KH, Ocampo AC, Ivanov BA. 1997. Energy, volatile production, and climatic effects of the Chicxulub Cretaceous/Tertiary impact. *J. Geophys. Res.* 102:21645–64

Rinehart JS, White WC. 1951. Shapes of craters formed in plaster of paris by ultra-speed pellets. *J. Appl. Phys.* 22:14–18

Roddy DJ. 1977. Large-scale impact and explosion craters: comparisons of morphological and structural analogs. In *Impact and Explosion Cratering*, ed. DJ Roddy, RO Pepin, RB Merrill, pp. 185–246. New York: Pergamon. 1301 pp.

Ryder G, Fastovsky D, Gartner S, eds. 1996. *The Cretaceous-Tertiary Event and Other Catastrophes in Earth History. Geol. Soc. Am. Special Paper* 307. Boulder, CO: Geol. Soc. Am. 569 pp.

Schaber GG, Strom RG, Moore HJ, Soderblom LA, Kirk RL, et al. 1992. Geology and distribution of impact craters on Venus: What are they telling us? *J. Geophys. Res.* 97:13257–301

Schmidt RM, Housen KR. 1987. Some recent advances in the scaling of impact and explosion cratering. *Int. J. Impact Eng.* 5:543–60

Schröter JH. 1791. *Selenotopographische Fragmente*, Vols. 1, 2. Göttingen: Lilienthal & Helmst

Schultz PH. 1992. Atmospheric effects on ejecta emplacement and crater formation on Venus from Magellan. *J. Geophys. Res.* 97:16183–248

Schultz PH. 1994. Chicxulub as an oblique impact. *Lunar Planet. Sci. Conf.* 25:1211–12

Schultz PH. 1995. Making the man in the moon: origin of the Imbrium Basin. *Lunar Planet. Sci. Conf.* 26:1251–52

Schultz PH. 1996a. Effect of impact angle on vaporization. *J. Geophys. Res.* 100:21117–35

Schultz PH 1996b. Nature of the Orientale and Crisium impacts. *Lunar Planet. Sci. Conf.* 26:1147–48

Schultz PH. 1997. Forming the South-Pole Aitken Basin: the extreme games. *Lunar Planet. Sci. Conf.* 28:1259–60

Schultz PH. 1999. Ejecta distribution from oblique impacts into particulate targets. *Lunar Planet. Sci. Conf.* 30, Abstr. #1919. Houston: Lunar Planet. Inst. (CD-ROM)

Schultz PH, Lutz-Garihan AB. 1982. Grazing impacts on Mars: a record of lost satellites. *Proc. Lunar Planet. Sci. Conf.* 13:A84–96

Schultz PH, Gault DE. 1990. Prolonged global catastrophes from oblique impacts. See Sharpton & Ward 1990, pp. 239–61

Schultz PH, Lianza RE. 1992. Recent grazing impacts on the Earth recorded in the Rio Cuarto crater field, Argentina. *Nature* 355:234–37

Schultz PH, Anderson RR. 1996. Asymmetry of the Manson impact structure: evidence for impact angle and direction. In *The Manson Impact Structure, Iowa: Anatomy of an Impact Crater*, Geol. Soc. Am. Spec. Pap. 302:397–417

Schultz PH, D'Hondt S. 1996. Cretaceous-Tertiary (Chicxulub) impact angle and its consequences. *Geology* 24:963–67

Schultz PH, Sugita S. 1997. Fate of the Chicxulub impactor. *Lunar Planet. Sci. Conf.* 28:1261–62

Schultz PH, Koeberl C, Bunch T, Grant J, Collins W. 1994. Ground truth for oblique impact processes: new insight from the Rio Cuarto, Argentina, crater field. *Geology* 22:889–92

Sepkoski J. 1994. Extinction and the fossil record. *Geotimes* 39:15–17

SESAME '83. 1983. *Report on the Los Alamos Equation-of-State Library. LALP-83–4.* Los Alamos, NM: Los Alamos Natl. Lab.

Sharpton VL, Ward PD, eds. 1990. *Global Catastrophes in Earth History: An Interdisciplinary Conference on Impacts, Volcanism, and Mass Mortality. Geol. Soc. Am. Special Paper 247.* Boulder, CO: Geol. Soc. Am. 631 pp.

Shoemaker EM. 1962. Interpretation of lunar craters. In *Physics and Astronomy of the Moon,* ed. Z Kopal, pp. 283–359. New York/London: Academic. 538 pp.

Shoemaker EM. 1977. Why study impact craters? In *Impact and Explosion Cratering,* ed. DJ Roddy, RO Pepin, RB Merrill, pp. 1–10. New York: Pergamon. 1301 pp.

Smits EI, Sanchez AG. 1973. Fresh lunar craters: morphology as a function of diameter, a possible criterion for crater origin. *Mod. Geol.* 4:51–59

Stöffler D, Gault DE, Wedekind FJ, Polkowski G. 1975. Experimental hypervelocity impact into quartz sand: distribution and shock metamorphism of ejecta. *J. Geophys. Res.* 80:4062–77

Strom RG, Croft SK, Barlow NG. 1992. The Martian impact cratering record. In *Mars,* ed. HH Kieffer, BM Jakosky, CW Snyder, MS Matthews, pp. 383–423. Tucson-London: Univ. Ariz. Press. 1498 pp.

Vickery AM. 1986. Effect of an impact-generated gas cloud on the acceleration of solid ejecta. *J. Geophys. Res.* 91:14139–60

Walker D, Stolper EM, Hays JF. 1979. Basaltic volcanism: the importance of planet size. *Proc. Lunar Planet. Sci. Conf.* 10:1995–2015

Wasson JT, Wetherill GW. 1979. Dynamical, chemical and isotopic evidence regarding the formation locations of asteroids and meteorites. In *Asteroids,* ed. T Gehrels, pp. 926–74. New York: Pergamon 1181 pp.

Wilhelms DE. 1987. *The Geologic History of the Moon. U.S. Geol. Survey Prof. Pap. 1348.* Washington, DC: US Gov. Print. Off. 328 pp.

Wilhelms DE. 1992. *To a rocky Moon: a geologist's history of lunar exploration.* Tucson-London: Univ. Ariz. Press. 477 pp.

Witzke BJ, Hammond RH, Anderson RR. 1996. Deposition of the Crow Creek Member, Campanian, South Dakota and Nebraska. In *The Manson Impact Structure, Iowa: Anatomy of an Impact Crater,* Geol. Soc. Am. Spec. Pap. 302: 433–56

Annual Review of Earth and Planetary Science
Volume 28, 2000

CONTENTS